Int. J. Heat Mass Transfer. Vol. 36, No. 9, pp. 2261–2270, 1993
Printed in Great Britain

0017-9310/93 $6.00 + 0.00

A unified model for the prediction of bubble detachment diameters in boiling systems—I. Pool boiling

L. Z. ZENG, J. F. KLAUSNER and R. MEI†
University of Florida, Department of Mechanical Engineering, Gainesville, FL 32611, U.S.A.

(*Received* 8 *June* 1992 *and in final form* 30 *November* 1992)

Abstract—A new model is proposed for the prediction of vapor bubble departure diameters in saturated pool boiling. The model utilizes a force balance which follows a similar form as that used by Klausner *et al.* (*Int. J. Heat Mass Transfer* **36**, 651–662 (1993)) for flow boiling. The vapor bubble growth rate is a necessary input to the model, and its reliable estimation is required to predict accurately departure diameters. The model has been tested over the following range of conditions: pressure, 0.02–2.8 bar; Jakob number, 4–869; and gravity, 1–0.014 g. It is demonstrated that over the wide range of boiling data considered the departure diameter predicted using the present model is significantly improved over existing correlations.

1. INTRODUCTION

NUMEROUS correlations have been proposed for the prediction of bubble detachment diameters in pool boiling [1–13]. An excellent summary of many of these models is given by Cole and Shulman [9]. Recently, Klausner *et al.* [14] demonstrated that in flow boiling systems vapor bubbles typically detach from the nucleation site via sliding and lift off the heating surface downstream of the nucleation site. The instant at which a vapor bubble detaches from the nucleation site was referred to as the point of departure and the instant they detach from the heating surface was referred to as the lift-off point. In pool boiling systems the departure and lift-off points coincide and for the remainder of this work will be referred to as the departure point. The basis for the majority of pool boiling vapor bubble departure correlations is the supposition that at the point of departure the net force acting on the bubble is zero. It has generally been assumed that the dominant forces are those due to gravity and surface tension. Some investigators have also attempted to account for the force due to bubble growth [3, 6, 9].

The surface tension force acting on a growing vapor bubble in pool boiling, such as that shown in Fig. 1, is given by

$$F_{sy} = -\pi d_w \sigma \sin \alpha \qquad (1)$$

where d_w is the contact diameter, σ is the surface tension coefficient, and α is the contact angle. Many believe that the main obstacle which has prevented the development of a generally valid expression for the departure diameter is an inability to predict d_w, and α. According to Cooper and Chandratilleke [15], Cooper *et al.* [16], and Zysin *et al.* [17], the contact diameter at the base of a growing bubble embedded in a superheated thermal layer is not easily measured. There exists an index of refraction gradient in the thermal boundary layer which creates a mirage of the bubble near its base. Therefore, those investigators who relied on visual measurements without taking into account this phenomenon will have severely overestimated the contact diameter as well as the surface tension force. The hypothesis by Moore and Mesler [18] that a liquid microlayer exists beneath a growing vapor bubble has been substantiated by various investigators and is discussed in detail by Cooper and Lloyd [19]. Due to the existence of the liquid microlayer it is probable that the contact diameter is 'very small'. Unfortunately, 'very small' is difficult to quantify because reliable measurements of the contact diameter are not currently available. Although the contact diameter continually changes during the growth cycle of a vapor bubble, it is reasonable to suggest that the

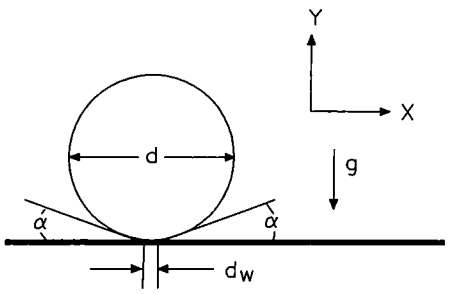

FIG. 1. Ideal pool boiling vapor bubble attached to horizontal heating surface.

†Department of Aerospace Engineering, Mechanics and Engineering Science.

NOMENCLATURE

a	vapor bubble radius [m]
C_D	drag coefficient
C_{pl}	liquid specific heat [J kg^{-1} K^{-1}]
C_s	empirical constant equal to 20/3; modifies growth force
d	vapor bubble departure diameter [m]
d_w	vapor bubble contact diameter [m]
F	force [N]
g	gravity [m s^{-2}]
h_{fg}	latent heat of vaporization [J kg^{-1} K^{-1}]
Ja	Jakob number
t	time [s]
ΔT_{sat}	wall superheat [°C]
u_b	velocity of bubble interface [m s^{-1}]
u_{bcy}	velocity of vapor bubble center of mass [m s^{-1}]
V_b	vapor bubble volume.

Greek symbols

α	liquid/vapor contact angle
η	liquid thermal diffusivity [m^2 s^{-1}]
ρ	density [kg m^{-3}].

Subscripts

l	liquid
v	vapor.

contact diameter approaches zero near the point of departure due to the necking phenomenon which has been clearly identified by Jakob [20], Van Stralen *et al.* [21], and Johnson *et al.* [22]. The computational study of Lee and Nydahl [23] predicts that the surface tension force is an order of magnitude less than the buoyancy and growth forces near the departure point. Therefore, the approach taken in this work is to assume the surface tension force approaches zero at the point of departure. It is emphasized that this assumption does not imply the surface tension force is in general negligible. In fact, just prior to bubble growth, it is the surface tension force which adheres the bubble to the heating surface. Also, if conditions arise where the growth rate is very small, it is possible for the surface tension force to be of the same order of magnitude as the growth force. It is only near the point of departure that the assumption of a small surface tension force is being employed. Therefore, the physical basis for the present model is that at the point of departure the buoyancy force is balanced by the growth force as opposed to the surface tension force as has been previously assumed by many investigators.

2. DEPARTURE DIAMETER MODEL

The growth and departure of vapor bubbles from a solid heating surface is a dynamic process for which the momentum and energy exchange between the growing bubble and the surrounding liquid must be considered. The momentum equation for a growing bubble in the direction normal to a horizontal heating surface (y-direction) may be expressed as

$$\sum F_y = F_{sy}+F_{duy}+F_b+F_{cp}+F_L = \rho_v V_b \frac{du_{bcy}}{dt} \quad (2)$$

where F_{sy} is the surface tension force, F_{duy} is the unsteady growth force, F_b is the buoyancy force, F_{cp} is the contact pressure force, F_L is the lift force created by the wake of the preceding departed vapor bubble, ρ_v is the vapor density, V_b is the bubble volume, u_{bcy} is the velocity of the center of mass of the bubble, and t denotes time. With the exception of F_L, a complete derivation of these forces and illustrations on how they may be estimated were given by Klausner *et al.* [14]. A gross estimation for F_L is given in the Appendix. The right hand side of (2) represents the acceleration of the vapor bubble and for most cases of practical interest is negligibly small while the bubble is attached to the heating surface because du_{bcy}/dt is finite at the point of departure and $\rho_v/\rho_l \ll 1$. Therefore, should the quasi-static condition that $\Sigma F_y = 0$ be violated, the vapor bubble will depart the heating surface.

In order to obtain a useful vapor bubble departure model it is important to identify which of those forces acting on a growing bubble are dominant. As was mentioned above, the surface tension force can be assumed to be negligible at the point of departure. Direct proof of this hypothesis is currently lacking, and thus the usefulness of the proposed vapor bubble departure model can only be judged based on comparison with available experimental departure data. In addition, it is demonstrated in the Appendix that F_L is generally negligible for boiling systems. The buoyancy and contact pressure forces are respectively given by

$$F_b = V_b(\rho_l-\rho_v)g \quad (3)$$

$$F_{cp} = \frac{\pi d_w^2}{4}\frac{2\sigma}{r_r} \quad (4)$$

where g is the gravitational acceleration, ρ_l the liquid density, and r_r the radius of curvature at the base of the bubble. Photographs of growing vapor bubbles from Van Stralen *et al.* [21] suggest $d_w/r_r \ll 1$, and it is clear that the contact pressure force may be

neglected at the point of departure since it is small compared to the surface tension force given in (1). Thus vapor bubble departure will occur when F_b+F_{duy} exceeds zero. It is worthwhile mentioning that Ruckenstein [5] and Roll and Meyers [13] arrived at the same conclusion. Ruckenstein [5] estimated the growth force from,

$$F_{duy} = -C_D\pi a^2\rho_l\frac{u_b^2}{2}$$

and Roll and Meyers [13] used,

$$F_{duy} = -C_D\pi a^2\rho_l\frac{u_b^2}{2} - \tfrac{2}{3}\pi a^3(1+\tfrac{3}{8})\dot{u}_b$$

where a is the bubble radius, u_b, the bubble velocity, was taken to be $2\dot{a}$, and $(\dot{})$ denotes differentiation with respect to time. Ruckenstein [5] assumed C_D was unity while Roll and Meyers [13] evaluated C_D from experimental data for freely rising bubbles in liquid. However, neither the bubble departure correlation of Ruckenstein [5] nor Roll and Meyers [13] accurately predicts vapor bubble departure diameters.

Klausner *et al.* [14] modelled the growth force by considering a hemispherical bubble expanding in an inviscid liquid. Here, the same form of the growth force will be utilized except that an empirical constant, C_s, is introduced which attempts to primarily account for the presence of a wall,

$$F_{duy} = -\rho_l\pi a^2(\tfrac{3}{2}C_s\dot{a}^2+a\ddot{a}). \quad (5)$$

Based on 190 pool boiling data points considered herein, it has been found that $C_s = 20/3$ gives the best fit to the bubble departure data based on a least squares regression analysis. Although equation (5) provides excellent agreement with the data, it is recognized that it is only an approximation of the growth force based on a finite number of experimental data sets, and there exists room for improved modelling.

In order to evaluate the growth force, the vapor bubble growth rate, $a(t)$, is required. The theoretical determination of $a(t)$ must include the detailed analysis of both momentum and energy transfer between the liquid and vapor phase. This approach is too complex, and the determination of $a(t)$ based on empiricism is used here instead. In general the vapor bubble growth rate follows a power law

$$a(t) = Kt^n \quad (6)$$

where K and n are determined empirically. Equation (6) is useful in evaluating the growth force only when specific information on the vapor bubble growth rate is available. When the bubble growth rate is expressed in the general form given by (6), F_{duy} can be expressed as

$$F_{duy} = -\rho_l\pi K^{2/n}[\tfrac{3}{2}C_sn^2+n(n-1)]a^{4-(2/n)}. \quad (7)$$

The balancing of F_{duy} by F_b results in

$$d = 2\left\{\frac{3}{4}\frac{K^{2/n}}{g}[\tfrac{3}{2}C_sn^2+n(n-1)]\right\}^{n/(2-n)} \quad (8)$$

where d is the departure diameter and $\rho_v/\rho_l \ll 1$ has been assumed. An immediate result of (8) is that when $g \to 0$ the vapor bubbles will not depart the heating surface unless there is some external mechanism to induce an inertial force, such as system vibration. The zero-gravity pool boiling photographs provided by Siegel and Usiskin [24] tend to support this analysis.

When no specific information about bubble growth rate is available, the diffusion controlled bubble growth solution proposed by Zuber [25] is most useful for boiling under one-g subatmospheric and atmospheric pressure conditions

$$a(t) = \frac{2b}{\sqrt{\pi}}Ja\sqrt{(\eta t)} \quad (9)$$

where

$$Ja = \frac{\rho_l C_{pl}\Delta T_{sat}}{\rho_v h_{fg}}.$$

Ja is the Jakob number, η the liquid thermal diffusivity, C_{pl} the liquid specific heat, h_{fg} the latent heat of vaporization, ΔT_{sat} the wall superheat, and b is an empirical constant which is supposed to account for asphericity of the growing vapor bubble and typically lies between 1 and $\sqrt{3}$. It is noted that equation (9) is only an approximation of the bubble growth rate. For vapor bubbles growing in a nonuniform temperature field Griffith [26] has shown that as the Jakob number, Ja, decreases both K and n in equation (6) decrease. Therefore, as pressure increases the vapor bubble growth rate decreases. Unfortunately, Griffith's [26] analysis is not currently useful as a predictive tool since knowledge of the thermal boundary layer thickness is required but is not available. In addition, Strenge *et al.* [27] measured growth rates from a single nucleation site and found that values of n varied from 0.312 to 0.512 in an ensemble of 86 bubbles. Caution must be exercised when applying equation (9) to a single observation of bubble growth. It is seen that the driving potential for bubble growth is the wall superheat. Recently, Kenning [28] demonstrated that for pool boiling systems, the local wall superheat can vary by as much as 150% over the heating surface. Therefore, the wall superheat controlling the growth of vapor bubbles at a specific nucleation site is not likely to be the mean wall superheat, which is what is typically measured by most investigators. Therefore variations in measured values of b may also be attributed to the nonuniform temperature field on the heating surface. Despite these shortcomings, equation (9) is utilized for subatmospheric and atmospheric pressure pool boiling, where b is determined from the measured growth rate corresponding to each measured departure diameter. Based on the limited available experimental data considered herein, the estimated mean values for b are summarized in Table 1,

Table 1. Empirically determined values of b to be used with equation (9)

Boiling liquids	Pressure (bar)	Wall superheat (°C)	Ja	b	Relative STDV†
Acetone [9]	0.3–0.6	27.0	16	5.37	0.335
Aqueous-sucrose sol. [30]	1.0	17.0	50	19.57	0.091
Carbon tetra. [9]	0.2	28.0	4	24.24	0.402
Methanol [9]	0.2–0.7	18.0–28.0	30–46	1.57	0.299
Methanol [3]	1.0	14.0–19.0	19–26	0.82	0.317
n-Pentane [9]	0.7	28.0	46	0.52	0.154
n-Pentane [9]	1.0	17.0	28	1.22	0.167
Toluene [9]	0.06	13.0	11	14.60	0.218
Water [9, 21]	0.02–0.5	15.0–23.0	88–869	0.48	0.500
Water [3, 31, 32]	1.0	10.0	31	0.86	0.430

†Relative STDV is the standard deviation of b normalized by the mean.

which should be useful for estimating the mean vapor bubble growth rate for a given ΔT_{sat}.

3. COMPARISON OF DEPARTURE MODEL WITH EXPERIMENTAL DATA

The condition that $F_b + F_{duy} > 0$ is the criteria used for vapor bubble departure. The manner in which F_b and F_{duy} are evaluated is mentioned above. Since the growth force is dependent on the vapor bubble growth rate, vapor bubble departure data sets were only considered if both departure diameter and growth rate data were specified. The available data from the literature were subdivided into four categories: subatmospheric pressure, atmospheric pressure, elevated pressure, and reduced gravity. The various fluids, pressure range, and gravitational field for the bubble departure data considered as well as their source are summarized in Table 2. A useful statistic referred to here as the relative deviation (*r.d.*) is used to judge the performance of the present departure model against existing correlations, and is defined by

$$r.d. = \frac{\sum_{k=1}^{N} \frac{|d_{meas,k} - d_{pred,k}|}{d_{meas,k}}}{N} \times 100 \qquad (10)$$

where N is the number of data points, and the subscripts 'meas' and 'pred' refer to the respective measured and predicted departure diameters. It is emphasized that d_{pred} is based on the measured vapor bubble growth rate which corresponds to d_{meas}. Since d_{meas} is based solely on a single observation, as opposed to a mean value based on a large ensemble of observations as were reported by Klausner *et al.* [14], it would be inappropriate to use the mean values of b reported in Table 1 for calculating the growth rate.

3.1. *Subatmospheric pressure, earth gravity*

A comparison between the measured and predicted departure diameters for subatmospheric pressure, earth gravity pool boiling is shown in Fig. 2. For the 105 data points considered, which encompass six different fluids and span two orders of magnitude in departure diameter, the comparison is excellent. The relative deviation, displayed in Table 2, is 10%. It is also shown in Table 2 that the only other correlation which gives comparable predictions to the present model is that of Cole and Shulman [9], referred to as Cole and Shulman 2 in Table 2, for which the relative deviation is 29%. A comparison between the measured departure diameters and their model for subatmospheric pressure is displayed in Fig. 3. Their correlation represents an empirical fit of bubble departure data over a range of pressures. It is noted that in preparing Table 2, the present model is the only one in which measured bubble growth rate data were used to calculate departure diameters.

3.2. *Atmospheric pressure, earth gravity*

The atmospheric pressure, earth gravity pool boiling departure data are comprised of four different fluids and 67 data points. A comparison between the measured and predicted departure diameters using the present model is shown in Fig. 4. It is seen that the comparison is also excellent. The relative deviation shown in Table 2 is 15%. A comparison between the data and the Cole and Shulman 2 correlation is shown in Fig. 5. The Cole and Shulman 2 correlation which was satisfactory for subatmospheric pressure data is also adequate for atmospheric pressure data and has a relative deviation of 31%. However, when comparing Figs. 4 and 5, the present model appears more accurate. Besides the present model, the best correlations are those of Fritz [1] and Cole and Rohsenow [11] which have a relative deviation of 18%.

3.3. *Elevated pressure, earth gravity*

The elevated pressure and reduced gravity departure results are not conclusive since the number of data points available is small. Nevertheless, as long as the growth rate is specified satisfactory results can be obtained using the present model. For the elevated pressure data 11 departure diameter data points are available which have been obtained by Staniszewski [3] using two fluids. The pressure ranges from 1.9 to 2.8 atmospheres. The experimental growth rate data available are difficult to analyze since at certain times the bubble diameters appear to have a step increase.

Table 2. Mean deviation tabulated for present vapor bubble departure model as well as other departure correlations reported in the literature

Boiling conditions	Boiling liquids	Numbers of data points	This work	Fritz [1]	Zuber [2]	Staniszewski [3]	Nishikawa & Urakawa [4]	Roll & Myers [13]	Ruckenstein [5]
Sub-atmospheric pressure one-g	Acetone [9]	15	6.8	80.9	85.2	67.8	36.5	81.5	85.1
	Carbon Tetra. [9]	10	7.3	83	86.5	73.3	57.1	99.2	98.1
	Methanol [9]	43	9.8	73	76.3	63.5	26.3	34.9	38.6
	n-Pentane [9]	5	18.5	23.7	43.7	28	127.1	167.9	118.3
	Toluene [9]	5	9.2	94.5	94.6	87	21.3	98.7	97
	Water [9, 21]	27	11.9	90.5	90.9	81.7	57.1	372.1	279
	Combined	105	10	78.3	81.6	69.2	43.2	143.7	119.3
atmospheric pressure one-g	Methanol [3]	8	18.9	16.3	52.2	8.8	157.1	33.9	31.6
	n-Pentane [9]	2	14.8	28.6	54.3	29.1	69.6	36.9	26.9
	Aqueous-sucrose sol. [30]	6	14.7	30.7	44.5	66.5	11.1	555.0	140.4
	Water [3, 31, 32]	51	14.9	16.9	56.8	34.2	43.6	138.4	94.1
	Combined	67	15.3	18.4	55.1	33.9	55	160.2	88.8
elevated pressure one-g	Methanol [3]	3	17.3	55	37.5	15.6	156	85.6	67
	Water [3]	8	28.8	39.9	41.5	18.5	47.7	51.0	33.6
	Combined	11	25.7	44.1	40.4	17.7	77.3	60.4	42.7
one-atm micro-g	Aqueous-sucrose solution [30]	5	16.2	106.7	33.7	49.4	14.5	440.4	345

Subatmospheric pressure range: 0.02–0.7 bar.
Elevated pressure range: 1.9–2.8 bar.
Micro-g range: 0.014–0.43 g.

Table 2.—*Continued.*

Boiling conditions	Boiling liquids	Han & Griffith [6]	Semeria 1 [7]	Semeria 2 [8]	Cole & Shulman 1†	Cole & Shulman 2‡	Cole [10]	Cole & Rohsenow [11]	Kocamustafaogullari [12]
Sub-atmospheric pressure one-*g*	Acetone [9]	76.1	69.2	547.1	16.3	32.6	86.9	93.7	91.8
	Carbon Tetra. [9]	185.5	52.2	2167	27.8	54.4	97.4	99.2	95.8
	Methanol [9]	140.9	57.5	691.4	25.6	16.1	59.3	64.1	86.5
	n-Pentane [9]	198.5	7.6	963.4	57.4	56.2	49.4	12.7	85.9
	Toluene [9]	13.4	71.8	3265	46.4	66.2	96.6	96.4	99.2
	Water [9, 21]	34.3	83.5	845.8	31.1	29.6	43.6	30.6	58.4
	Combined	105.2	63.7	986.5	28.4	29	64.1	62.2	81.5
atmospheric pressure one-*g*	Methanol [3]	371.3	20.2	753.1	116.8	49.5	13.6	20.7	57.6
	n-Pentane [9]	235.1	25.3	462.9	59.1	6	39.1	43.8	89.9
	Aqueous-sucrose sol. [30]	130.5	52.7	256.8	30.7	6.6	48.4	21.1	32.6
	Water [3, 31, 32]	110.8	38	366.8	73.2	31.7	38.6	16.6	17.6
	Combined	147.4	36.8	406	74.1	30.8	36.5	18.3	25.9
elevated pressure one-*g*	Methanol [3]	339	26.3	333.7	110.1	32.2	63.7	29.8	69.1
	Water [3]	91.3	32	155	86.5	22.7	34.3	33.8	30.5
	Combined	158.8	30.5	204.1	93	25.3	42.3	32.7	41.0
one-atm micro-*g*	Aqueous-sucrose solution [30]	283.1	61	194.1	106.7	186.9	336.8	132.3	102.0

Subatmospheric pressure range: 0.02–0.7 bar.
Elevated pressure range: 1.9–2.8 bar.
Micro-*g* range: 0.014–0.43 g.
†Corresponds to equation (31) in ref. [9].
‡Corresponds to equation (29) in ref. [9].

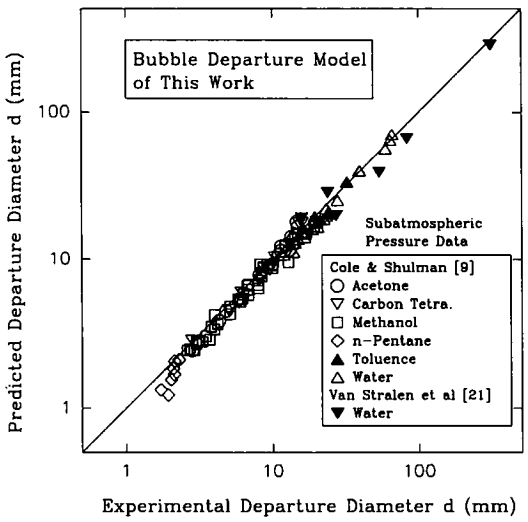

FIG. 2. Comparison of predicted and measured vapor bubble departure diameter for subatmospheric pressure data using present model.

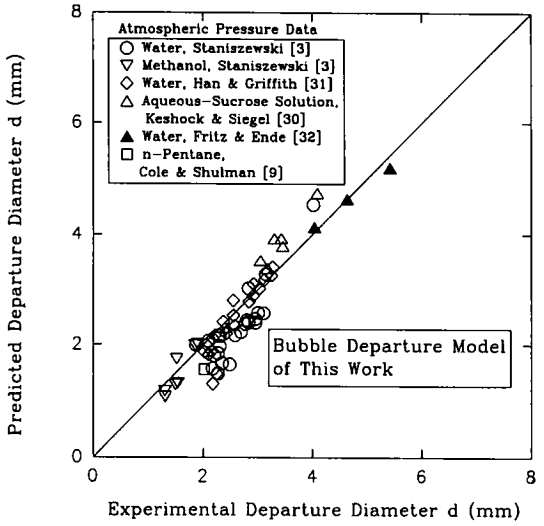

FIG. 4. Comparison of predicted and measured vapor bubble departure diameter for atmospheric pressure data using present model.

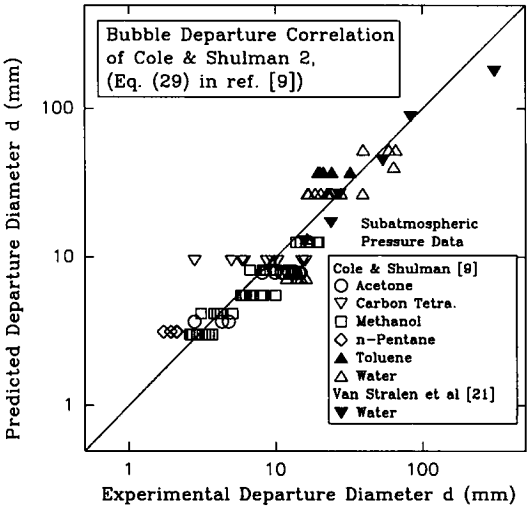

FIG. 3. Comparison of predicted and measured vapor bubble departure diameter for subatmospheric pressure data using Cole and Shulman 2 correlation.

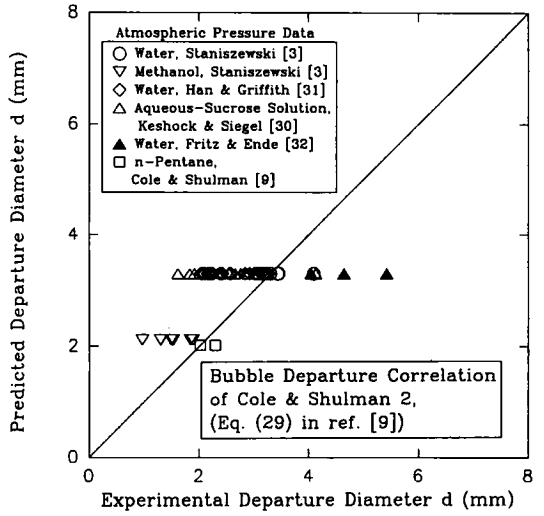

FIG. 5. Comparison of predicted and measured vapor bubble departure diameter for atmospheric pressure data using Cole and Shulman 2 correlation.

Nevertheless, equation (6) is used for specifying the growth rate, and the predicted departure diameters are compared with the measured values in Table 3. Also shown in Table 3 are the experimentally determined values for K and n to be used with equation (6). It is seen that at elevated pressures the values for n range from 0.24 to 0.38 which represents a decrease in bubble growth rate. This trend is in agreement with Griffith's [26] bubble growth model. As is seen from Table 2, the relative deviation for this set of data using the present model is 26%, which is high compared to the subatmospheric and atmospheric pressure data. The best correlation is that of Staniszewski [3] in which the relative deviation is 18%. The relative deviation for the Cole and Shulman 2 correlation is 25%. It is interesting to note that since the vapor bubble growth rate decreases with increasing pressure, the present model predicts that the departure diameter should decrease with increasing pressure, under otherwise similar conditions. The elevated pressure bubble departure data of Tolubinsky and Ostrovsky [29] definitively support this prediction. Unfortunately, their data does not provide enough information for comparison against the present bubble departure model because growth rate data were not specified.

3.4. *Reduced gravity*

For the reduced gravity data, five data points are available in which the gravitational field varies from

Table 3. Comparison of measured and predicted vapor bubble departure diameter for elevated pressure data using present model

Boiling liquids	System pressure (bar)	Depart. diam. measured (mm)	Depart. diam. predicted (mm)	K†	n
Water	1.93	2.20	1.43	0.00444	0.38
		1.58	1.12	0.00388	0.37
		1.41	1.10	0.00254	0.29
		1.86	1.30	0.00259	0.26
		1.13	1.18	0.00202	0.22
		1.73	1.27	0.00209	0.24
	2.76	1.83	1.07	0.00301	0.34
		1.77	1.04	0.00282	0.33
Methanol	1.93	1.24	1.03	0.00250	0.30
		0.69	0.57	0.00256	0.38
	2.76	1.01	0.83	0.00216	0.31

†Units on K are such that when applied to equation (6) the radius dimension is meters.

Table 4. Comparison of measured and predicted vapor bubble departure diameter for reduced gravity data using present model

Percentage of earth gravity	Depart. diam. measured (mm)	Depart. diam. predicted (mm)	K†	n
42.9	3.84	4.50	0.00993	0.42
22.9	3.79	3.28	0.00430	0.22
12.6	4.90	5.63	0.00932	0.37
6.1	3.38	3.87	0.00605	0.36
1.4	5.21	6.28	0.00552	0.22

†Units on K are such that when applied to equation (6) the radius dimension is meters.

0.014 to 0.43 of earth gravity. These data indicate that the vapor bubble growth rate decreases with decreasing gravity. Table 4 displays the predicted departure diameters using the current model compared with the measured values as well as the values for K and n to be used with equation (6). It is seen that n decreases with decreasing gravitational field. For these five data points the relative deviation is 16%. The present correlation is the only one which satisfactorily correlates the reduced gravity data, besides that of Nishikawa and Urakawa [4].

4. CONCLUDING REMARKS

As highlighted in Table 2, the present vapor bubble departure model is the only one which is in satisfactory agreement with the measured bubble departure data over the entire range of boiling conditions considered. The good agreement between the measured and predicted departure diameters certainly lends credence to the hypothesis that the growth force is dominant compared to the surface tension force near the point of departure. The bounds of validity of this hypothesis have yet to be determined. Virtually every mechanistic pool boiling heat transfer correlation requires information on the vapor bubble departure diameter. The fact that pool boiling heat transfer correlations are only useful over a limited range of boiling conditions may be partially because most previously reported vapor bubble departure correlations fail to correlate adequately the data over a wide range.

The ultimate goal of this work is to provide a useful pool boiling vapor bubble departure model. Because the vapor bubble growth rate is required as an input to the model, it is currently only useful for predicting the average behavior of vapor bubble departure diameters under subatmospheric and atmospheric pressure boiling conditions, where the mean vapor bubble growth rate can be reasonably well estimated using equation (9). It is not currently possible to predict adequately the vapor bubble growth rate for elevated pressure and reduced gravity boiling, and therefore the present vapor bubble departure model will only be useful if an adequate growth rate model or correlation is developed for those conditions. Since many industrial boiling processes occur at elevated pressures, it is apparent that there should be a strong emphasis placed on understanding the influence of pressure or gravitational field on vapor bubble growth processes in future research endeavors.

Acknowledgements—This material is based on work supported by the National Science Foundation under Grant No. CTS-9008269.

REFERENCES

1. W. Fritz, Berechnung des maximalvolumens von dampfblasen, *Physik. Zeitschr* **36**, 379–384 (1935).
2. N. Zuber, Hydrodynamic aspects of boiling heat transfer, U.S. AEC Rep. AECU 4439, Tech. Inf. Serv., Oak Ridge, Tenn. (1959).
3. B. E. Staniszewski, Bubble growth and departure in nucleate boiling, Tech. Rept. No. 16, MIT, Cambridge, Mass. (1959).
4. K. Nishikawa and K. Urakawa, An experiment of nucleate boiling under reduced pressure, *Mem. Fac. Engng Kyushu Univ.* **19**, 63–71 (1960).
5. E. Ruckenstein, A physical model for nucleate boiling heat transfer from a horizontal surface, *Bul. Institutului Politech. Bucaresti* **33**(3), 79 (1961); AMR 16 (1963), Rev. 6055.
6. C. Y. Han and P. Griffith, The mechanism of heat transfer in nucleate pool boiling, Rept. 7613-19, MIT, Cambridge, Mass. (1962).
7. R. Semeria, Une méthode de détermination de la population de centres générateurs de bulles sur une surface chauffante dans l'eau bouillante, *Comptes Rendus, De L'Academie Des Sciences, Paris* **252**, 675–677 (1961).
8. R. Semeria, Caractéristiques des bulles de vapeur sur une paroi chauffante dans l'eau en ébullition à haute pression, *Comptes Rendus, De L'Academie Des Sciences, Paris* **256**, 1227–1230 (1963).
9. R. Cole and H. L. Shulman, Bubble departure diameters at subatmospheric pressures, *Chemical Engineering Progress Symposium Series* **62**(64), 6–16 (1966).
10. R. Cole, Bubble frequencies and departure volumes at subatmospheric pressures, *A.I.Ch.E. Jl* **13**, 779–783 (1967).
11. R. Cole and W. M. Rohsenow, Correlation of bubble departure diameters for boiling of saturated liquids, *Chemical Engineering Progress Symposium Series* **65**(92), 211–213 (1969).
12. G. Kocamustafaogullari, Pressure dependence of bubble departure diameter for water, *Int. Comm. Heat Mass Transfer* **10**, 501–509 (1983).
13. J. B. Roll and J. E. Myers, The effect of surface tension on factors in boiling heat transfer, *A.I.Ch.E. Jl* **10**, 530–534 (1964).
14. J. F. Klausner, R. Mei, D. M. Bernhard and L. Z. Zeng, Vapor bubble departure in forced convection boiling, *Int. J. Heat Mass Transfer* **36**, 651–662 (1993).
15. M. G. Cooper and T. T. Chandratilleke, Growth of diffusion-controlled vapor bubbles at a wall in a known temperature gradient, *Int. J. Heat Mass Transfer* **24**, 1475–1492 (1981).
16. M. G. Cooper, K. Mori and C. R. Stone, Behavior of vapor bubbles growing at a wall with forced flow, *Int. J. Heat Mass Transfer* **26**, 1489–1507 (1983).
17. L. V. Zysin, L. A. Fel'Dberg, A. L. Dobkes and A. G. Sazhenin, Allowance for optical distortion produced by temperature gradients in investigating the shape of vapor bubbles generated on a flat wall, *Heat Transfer—Sov. Res.* **12**(2), 6–10 (1980).
18. F. M. Moore and R. B. Mesler, The measurement of rapid surface temperature fluctuations during nucleate boiling of water, *A.I.Ch.E. Jl* 7(4), 620–624 (1961).
19. M. G. Cooper and A. J. P. Lloyd, The microlayer in nucleate pool boiling, *Int. J. Heat Mass Transfer* **12**, 895–913 (1969).
20. M. Jakob, *Heat Transfer*, Vol. 1. Wiley, New York (1959).
21. S. J. D. Van Stralen, R. Cole, W. M. Sluyter and M. S. Sohal, Bubble growth rates in nucleate boiling of water at subatmospheric pressures, *Int. J. Heat Mass Transfer* **18**, 655–669 (1975).
22. M. A. Johnson, Jr., Javier De La Peña and R. B. Mesler, Bubble shapes in nucleate boiling, *A.I.Ch.E. Jl* **12**(2), 344–348 (1966).
23. R. C. Lee and J. E. Nydahl, Numerical calculation of bubble growth in nucleate boiling from inception through departure, *J. Heat Transfer* **111**, 474–479 (1989).
24. R. Siegel and C. Usiskin, A photographic study of boiling in the absence of gravity, *J. Heat Transfer ASME Transactions* **81**(3), 230–236 (1959).
25. N. Zuber, The dynamics of vapor bubbles in nonuniform temperature fields, *Int. J. Heat Mass Transfer* **2**, 83–98 (1961).
26. P. Griffith, Bubble growth rates in boiling, *ASME Transactions* **80**, 721–727 (1958).
27. P. H. Strenge, A. Orell and J. W. Westwater, Microscopic study of bubble growth during nucleate boiling, *A.I.Ch.E. Jl* 7(4), 578–583 (1961).
28. D. B. R. Kenning, Wall temperature patterns in nucleate boiling, *Int. J. Heat Mass Transfer* **35**, 73–86 (1992).
29. V. I. Tolubinsky and J. N. Ostrovsky, On the mechanism of boiling heat transfer (vapor bubble growth rate in the process of boiling of liquids, solutions, and binary mixtures), *Int. J. Heat Mass Transfer* **9**, 1463–1470 (1966).
30. E. G. Keshock and R. Siegel, Forces acting on bubbles in nucleate boiling under normal and reduced gravity conditions, NASA Tech. Note TN D-2299, August (1964).
31. C. Y. Han and P. Griffith, The mechanism of heat transfer in nucleate pool boiling, part I: bubble initiation, growth and departure, *Int. J. Heat Mass Transfer* **8**, 887–904 (1965).
32. W. Fritz and W. Ende, Über den verdampfungsvorgang nach kinematographischen aufnahmen an dampfblasen, *Physik. Zeitschr* **37**, 391–401 (1936).
33. S. J. D. Van Stralen and R. Cole, *Boiling Phenomena*, Vol. 1. Hemisphere, New York (1979).
34. C.-H. Yih, *Fluid Mechanics*, p. 97. West River, Ann Arbor (1979).

APPENDIX: ESTIMATION OF WAKE INDUCED LIFT FORCE DUE TO A RISING BUBBLE

When a vapor bubble B is rising through a pool of liquid with velocity U in the vertical direction after it departs from the wall as shown in Fig. A1, it may induce a lift force on bubble A that remains attached to the wall and continues to grow. In order to obtain a gross estimation of that lift force, bubble A is modelled as a hemisphere with the same radius, a, as bubble B, and the liquid induced motion due to the rising bubble B is assumed to be inviscid. The center to center distance between bubbles A and B is H. Using the method of images by placing a bubble, B', at $y = -H$ with vertical velocity $-U$ and neglecting the effect of induced doublets

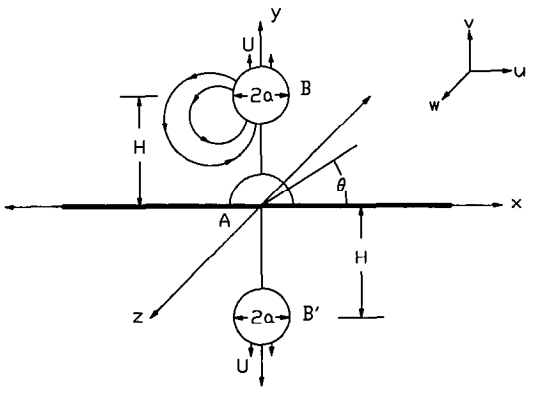

FIG. A1. Wake induced lift by rising bubble.

inside bubbles B and B', the velocity potential in the absence of bubble A to the leading order is

$$\phi(x,y,z) \approx -\frac{Ua^3}{2}\left[\frac{y-H}{[x^2+(y-H)^2+z^2]^{3/2}} - \frac{y+H}{[x^2+(y+H)^2+z^2]^{3/2}}\right]. \quad \text{(A1)}$$

For $H/a \gg 1$, the induced velocity field is, to the leading order for finite r/a,

$$u(x,y,z) \sim -3U\frac{a^3}{H^4}x$$

$$v(x,y,z) \sim +3U\frac{a^3}{H^4}y$$

$$w(x,y,z) \sim -3U\frac{a^3}{H^4}z \quad \text{(A2)}$$

where $r = (x^2+y^2+z^2)^{1/2}$ and u, v, and w are the velocity components in the respective x, y, and z directions. This velocity field describes a stagnation flow with the axis of symmetry being the y-axis. Placing the bubble A under this stagnation flow, the stream function can be found using Butler's theorem [34]. The velocity at the surface of bubble A due to this stagnation flow is found to be,

$$u_\theta = \frac{5}{2}\frac{3a^3}{H^4}Ua\sin\theta\cos\theta \quad \text{(A3)}$$

where θ is measured from the wall. Using Bernoulli's equation and referencing the pressure to $\theta = 0$ and $r = a$, which is consistent with the analysis of Klausner *et al.* [14], the lift force on bubble A is calculated by integrating the pressure around the surface

$$F_L = \frac{\rho_l}{2}\frac{25}{4}\frac{9a^6}{H^8}U^2a^2 2\pi a^2\int_0^{\pi/2}\sin^2\theta\cos^2\theta\sin\theta\cos\theta\,d\theta$$

$$= \tfrac{75}{16}\rho_l U^2 a^2\left(\frac{a}{H}\right)^8. \quad \text{(A4)}$$

In order to estimate F_L, it may be assumed that $U \sim 2\dot{a}$. Based on pool boiling photographs displayed by Van Stralen and Cole [33], a conservative estimate gives $(a/H) \sim (1/4)$. Thus, the ratio

$$\frac{F_L}{\rho_l \dot{a}^2 a^2} \sim \frac{75}{4}\frac{1}{4^8} \sim 2.86\times 10^{-4},$$

and when compared to the growth force given by equation (5), it is seen that the wake induced lift force is negligible for most cases of practical interest. One notable exception is when rising vapor jets follow the departure of a vapor bubble under certain subatmospheric pressure boiling conditions as has been discussed by Van Stralen *et al.* [21].